JOURNAL GEOLOGICAL SOCIETY OF INDIA
Vol.92, September 2018, pp.321-328

Methodological Validation for Automated Lineament Extraction by LINE Method in PCI Geomatica and MATLAB based Hough Transformation

Chalantika Laha Salui
Department of mining engineering, Indian Institute of Engineering Sciences and Technology, Shibpur, Howrah – 711 103, India
E-mail: *chalantikal@gmail.com*

ABSTRACT

Spatial distribution and pattern recognition of geologic lineaments are very effective in hazard risk evaluation. To make the process automated, various algorithms with various data sources were applied. This paper aims to make a review on such algorithms as well as data sources used. Comparative analysis of the LINE algorithm in PCI Geomatica and Hough Transformation in MATLAB has been conducted to explore the procedural accuracy with reference to existing landslides in the Darjeeling Himalayan region. Another comparison was made based on data sources like Landsat-8 OLI and digital elevation model, with reference to the same. As lineament density affects the landslide occurrences predominantly, the output lineament density by these two methods as well as with ground reflection and ground elevation data, were correlated with that of the landslide inventory map. A relational illustration was also done in between the lithological thrust direction and the direction of the individual lineament outputs. Hence, this study provides a decision on the use of a reliable method and data source for the automated lineament extraction which can be considered as generating an output with higher accuracy and, hence, safer for using it in the structural planning and execution of projects on various natural hazard studies.

INTRODUCTION

Lineaments are linear or curvilinear features on the earth's surface that give the expressions of under-lying geological structure. These are mainly geologic or tectonically weaker zones. It may be evident on the surface as geomorphologically contrasting feature in a linear pattern. They may be an expression of joints, faults and other line of weaknesses. Hobbs (1911) considered lineaments as results of zone of weakness or structural displacements in the crust of the earth. They can be traced as (1) shear zones/faults; (2) rift valleys; (3) truncation of outcrops; (4) fold axial traces; (5) joint and fracture traces; (6) topographic, vegetation, soil tonal changes alignment etc (Gupta, 1991). Geomorphologic imprints such as structural ridges, cliffs, terraces and aligned segments of a valley are the expression of lineaments, which results in a drastic variation of vegetation, moisture content, soil or rock composition etc (Thannoun, 2013). So, the study on lineament extraction is needed for landslide risk assessment, mineral exploration, hot spring detection, hydro-geological research, ground water potentiality etc. Therefore, technique is highly appreciated in terms of detecting the anomaly or edge detection. Satellite images and aerial photographs are extensively used to identify lineaments for different purposes, such as defining geological structures and tectonic fabrics (Neawsuparp and Charusiri, 2004). Lineaments extraction has been attempted from aerial photograph as well as satellite imageries, as a discontinuity that is darker or lighter in color in differentiation with the surrounding area. This linear anomalies can be detected either by manual interpretation followed by some image processing techniques like image ration, image fusion, directional edge detection filtering etc or automatically using computer software and algorithms (Prasad et al., 2013; Morris, 1991).

A number of works have been conducted to extract lineament automatically by computer algorithm. Various researchers worked on this with various inputs. Some works were tried on recent satellite optical images like Landsat-8 OLI (Ibrahim et al., 2014; Thannoun, 2013; Ali Hassan et al., 2014; El-sawy, 2016), whereas, some researchers have found it suitable to take high resolution digital elevation model (DEM) as input. The second was used more, mostly followed by hill-shade analysis. Abarca (2006), Alhirmizy (2015) and Masoud et al., (2011) tried to get lineaments automatically or semi-automatically from high resolution DEM, mostly generated from contours. Prasad et al., (2013) used ASTER DEM whereas Shankar et al., (2016) used LIDAR for their analysis. A number of researchers used Hough Transformation (Karnieli et al., 1996; Wang and Howarth, 1990, Rahnama and Gloaguen, 2014; Argialas and Mavrantza, 2004) whereas in some case studies Multi Hill-shade Hierarchic Clustering (MHHC) was used (Šilhavý et al., 2016). Besides DEM, high resolution satellite images with height information also were taken as input (Kocal et al., 2004) followed by analysis similar to the case of DEM. In such studies, LINE (Lineament Extraction) module of PCI Geomatica was used. DEM, along with the Thematic Mapper (TM) and Enhanced Thematic Mapper (ETM) and ancillary data of the area were used by some researchers (Argialas et al., 2004 and Abdullah, 2013). Lineament extraction from only Landsat TM data was also tried to be executed by Dalati (2000) and Thannoun (2013). Rahnama and Gloaguen, in 2014, on the other hand, tried to extract lineament by developing program in Matlab using ETM of Landsat-7. Mankisch et al., (2007) used laser scanning data and conducted analysis in ESRI, GRASS and eCognition environment. LINE and Hough Transformation, both uses the Canny's edge enhancement algorithm (Canny, 1986). Other edge enhancement technique like EDISON on Landsat ETM+ was tried by researchers (Mavrantza and Argialas, 2004).

Though there are various methodologies, this work tried to execute the automated lineament extraction by LINE module in PCI Geomantica platform and Hough Transformation by MATLAB R2009a coding. In general, automatic lineament extraction methods are based on edge detection techniques that enhance the pixels at the edges on an image. This is followed by edge linking along pixels displaying similarities such as same edge geometry are used to find the best fit of a known shape. The Hough transform method is a very robust technique for identifying and linking edge pixels that corresponds to linear features (Cross et al., 1988). In this method, the straight line $y = mx + b$ can be represented as a point (b, m) in the parameter space. It will calculate the parameters rho and theta (r, θ) of associated pixels to form a straight line. The Standard Hough Transform (SHT)

0016-7622/2018-92-3-321/$ 1.00 © GEOL. SOC. INDIA | DOI: 10.1007/s12594-018-1015-6

uses the parametric representation of a line:

$$rho = x*cos(theta) + y*sin(theta)$$

The technique is based on a voting process where every point in the image votes for all the possible shapes, in this case lines, passing through these given points. An accumulator array stores the votes and the line with the maximum amount of votes is extracted as a real feature in the image. Wang and Howarth (1990) used this method to detect lineaments in satellite images. Fitton and Cox (1998) also adapted this technique to extract lineaments from geo-scientific images. They tested the algorithm using a satellite image and a photograph of a veined outcrop. The algorithm showed to be able to extract lineaments at different scales although not all linear features were recognized.

The algorithm LINE (Linear Extraction) in PCI-Geomatica runs in three phases: edge detection, thresholding and curve extraction. This paper ran this algorithm on a high resolution DEM as well as on the forward PCA (principal component analysis) data of Landsat-8 (OLI). Hough transformation was run on the 8th band of Landsat-8 (OLI) because this band is specifically useful for edge detection. The basic motive of getting lineament outputs through various methods is to make a comparative study to get the accuracy and validate it with the real world scenario in terms of landslides. Because, landslides belong to lithologically less resistant areas and lineaments are the expression of such geologically weak zones. That's why; landslides have deep correlation with lineament density. Enormous studies on landslide risk zonation involve lineament density as an active parameter (Anbalagan et al., 2015; Matori et al., 2012; Mandal et al., 2014).

STUDY AREA AND DATA USED

The study is in the landslide prone Darjeeling district district of West Bengal. The geographical coordinate of the district is 27º 3' N to 26º27' N Latitude 88º53' E to 87º59' E Longitude covering an area of 3,149 km^2 (Fig.1a). The hill areas of Darjeeling district are located within the Lesser-Himalayan and Sub-Himalayan belts of the Eastern Himalayas (Dash, 1947; Mishra, 2014, Acton, 2011). This is bounded by the Sikkim Himalaya in the north, the Bhutan Himalaya in the east and Nepal Himalaya in the west. The southern foothill belt is demarcated by a highly dissipated platform of terrace deposits extending along the east west axis. The inner belt is defined by a ridgeline stretching from the Darjeeling hill to the west and Kalimpong hill to the east, overlooking the southerly flowing Tista valley in between. Prominent rivulets contributing to the Rammam - Rangit basin, dissipate the northern slope of Darjeeling hills. According to Mallet (1875) and Audent (1935) the tectonic units are found to be in the reverse stratigraphic order, and are represented by Siwalik and Gondwana systems. Towards the inner Himalayas, the thrusted sheets of Daling and Darjeeling group of crystalline rocks succeed. The contact between different groups of rocks is represented by thrusts, dipping at high angles towards north (Fig.1b). The Darjeeling hill area is formed of comparatively recent structure that has a direct bearing on landslides. According to government record, (*http://darjeeling.gov.in/geography.html*) Kalimpong I, Kalimpong II and Rangli – Rangliot blocks are severely vulnerable to landslides. The rate of vulnerability is also high in Kurseong and some parts of Gorubathan blocks. But as a whole, the condition is critical in

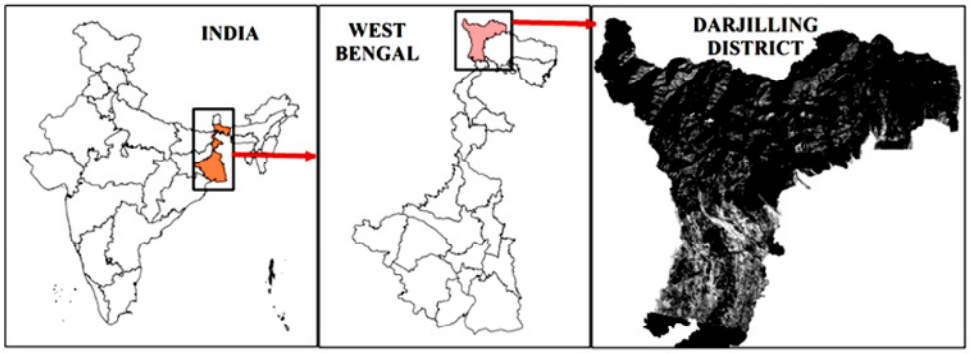

Fig.1a. Study area

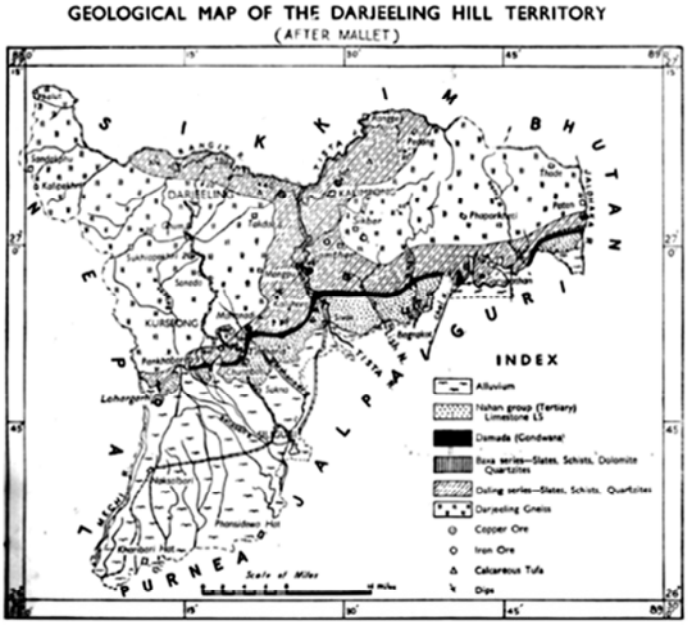

Fig.1b. Geology of the study area (source: Arthur Jules Dash, C.I.E., 1947).

Kalimpong sub-division, where the land under agriculture exceeds that of the area under plantation or forests.

The data covering this study area, used in the present work were: (a) Landsat-8 OLI (Operational Land Imager). It consists of 9 spectral bands with a spatial resolution of 30 m excluding band-8 which is 15 m. path-row index of the scene covering the full district is 139-041 acquired on 14th December, 2016. (b) Survey of India topographical sheets (partly 78A series and 78B series) covering whole Darjiling district on 1:50,000 scale. DEM was created based on digitized contour and spot height layers. (c) For the validation of individual method, existing landslide data was taken from the landslide inventory map by West Bengal Disaster Management Department website *(http://wbdmd.gov.in/Pages/Land_Mapping.aspx).*

METHODOLOGY

LINE Algorithm in PCI Geomatica

LINE algorithm was run on two datasets: Landsat-8 OLI and digital elevation model. But prior to use the module, data processing is needed. For the first one, the composite dataset was undergone the forward principal component analysis (PCA) and the first PCA image was taken due to its maximum information content.

For the second input, digital elevation data is required. Digital elevation model can be obtained from various sources like SRTM, ASTER etc. which are ready to use. But, for the purpose of avoiding data loss, the low interval contours of 40 m as well as the spot heights were digitized and used as inputs for DEM generation model ANUDEM (Topo to Raster I ArcGIS) (Zheng et al., 2016). Spot heights were added to avoid the artifacts like flat tops. The grid size values were determined from the total length of contours (Abarca., 2006). According to this, the grid resolution should be:

$$p = \frac{A}{2 * \Sigma l}$$

Where, p is the pixel size, A is the total study area and Σl is the total length of the contours within the area. In case of this study the calculation of p comes to approximately 30 m for interpolated grid size. The spline interpolation technique was chosen.

From the output DEM, eight shaded relief images were generated. They were derived in ArcGIS platform with light sources coming from eight different directions. The parameter of solar azimuth was taken as 00 and solar elevation as 300. Ambient light setting of 0.20 was used for a good contrasting output. So, the shaded relief images were created with four illumination directional angles of 180, 225, 270 and 315. Then they were overlaid to generate the input for automated lineament extraction through the LINE algorithm in PCI Geomatica.

This LINE algorithm run mainly considering several parameters like RADI (value taken as 12) which Specifies the radius of the edge detection filter, in pixels. This parameter roughly determines the smallest-detail level in the input image to be detected. GTHR, (value taken as 100) specifies the threshold in pixels for the minimum gradient level for an edge pixel. LTHR (value taken as 60) specifies the minimum length of curve, in pixels, to be considered as lineament or for further consideration; for example, linking with other curves. FTHR, (value taken as 10) specifies the maximum error, in pixels, allowed when fitting a polyline to a pixel curve. ATHR (value taken as 30) is the parameter which specifies the maximum angle, in degrees, between segments of a polyline. If the angle exceeds the specified maximum, the polyline is segmented into two or more vectors. This angle also defines the maximum angle between two vectors for them to be linked. DTHR (value taken as 20) Specifies the minimum distance, in pixels, between the end points of two vectors for them to be linked.

All these parameters involve in the process that is executed in three steps: edge detection, thresholding and curve extraction. In the first stage, the Canny's edge detection algorithm is applied to produce an edge strength image. The Canny edge detection algorithm has three sub-steps (*www.pcigeomatics.com/TrainingGuide-Geomatica-1.pdf*). First, the input image is filtered with a Gaussian function whose radius is provided by the RADI (Filter Radius) parameter. Then, the gradient is computed from the filtered image. Finally, pixels whose gradient are not the local maximum are suppressed by setting the edge strength to 0. In the second stage, the edge strength image is calibrated as per the threshold to obtain a binary image. Each ON pixel of the binary image represents an edge element. The threshold value is defined by the GTHR (Edge Gradient Threshold) parameter.

In the third stage, curves are extracted from the binary edge image. This step consists of several sub-steps. First, a thinning algorithm is applied to the binary edge image to produce pixel-wide skeleton curves. Then, a sequence of pixels for each curve is extracted from the image. Any curve with a number of pixels less than the value of the LTHR (Curve Length Threshold) parameter is discarded from further processing. An extracted pixel curve is converted to vector form by fitting line segments to it. The resulting polyline is an approximation of the original pixel curve, where the maximum fitting error (distance between the two) is specified by the FTHR (Line Fitting Threshold) parameter. Finally, the algorithm links pairs of polylines that satisfy the following criteria:

1. two end-segments of the two polylines face each other and have similar orientation (the angle between the two segment is less than the value specified by ATHR)
2. the two end-segments are close to each other (the distance between the end points is less than the value of DTHR)

Hough Transformation in MATLAB

The Hough transform is designed to detect collinear sets of edge pixels in an image by mapping these pixels into a parametric space or the Hough space (Hough, 1962, *https://in.mathworks.com/help/images/ref/hough.html?requestedDomain=in.mathworks.com*) defined in such a way that collinear sets of pixels in the image give rise to peaks in the Hough space (Duda et al., 1972; Ballard et al., 1982; Cross et al., 1988). For every line passing through (x_a, y_a), there would be a point in the mc space.

Any line passing through (x_a, y_a):

$$y_a = mx_a + c \text{ or } c = - x_a m + y_a$$

So, a point in the xy space is equivalent to a line in the mc space.

This parameterization specifies a straight line by the angle θ and the distance *p (rho)*. The equation of a line corresponding to this geometry is

$$\text{rho} = x*\cos(\text{theta}) + y*\sin(\text{theta})$$

If we restrict θ to the interval [0, n] , then the normal parameters for a line are unique. With this restriction, every line in the x-y plane corresponds to a unique point in the *θ-p* plane.

Suppose that we have a set { **((xl,** y l) , . . . , *(x,,, y ,)* }of *n* edge points, and we want to find a set of straight lines that fit them. We transform the points *(x,, y,*) into the sinusoidal curves in the *θ-p* plane described by

$$p = x, \cos \theta + yt \sin \theta$$

The variable *rho (ñ)* is the distance from the origin to the line along a vector perpendicular to the line. *Theta (θ)* is the angle of the perpendicular projection from the origin to the line measured in degrees clockwise from the positive *x*-axis. The range of *theta* is $-90° \leq \theta < 90°$. The angle of the line itself is *θ*+90°, also measured clockwise with respect to the positive *x*-axis (Fig.2).

Before analyzing the pixels in Hough platform, an edge detection

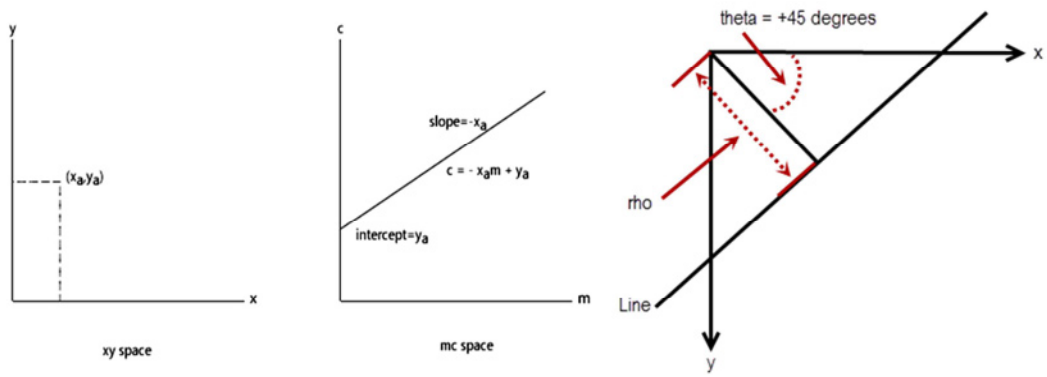

Fig.2. Paramentric character of a straight line.

algorithm is to be applied. So, here, Canny's edge detection (Canny, 1986) process was applied.

```
>>BW = edge (I,'canny');
```

BW — Binary image, specified as a real, 2-D, non-sparse logical or numeric array.

Calculate Hough transform.

```
>> [H,T,R] = hough(BW,'RhoResolution',0.5,
'ThetaResolution', 0.5);
```

Rho - Distance from the coordinate origin, specified as a real, 2-D, non-sparse logical or numeric array. The coordinate origin is the top-left corner of the image (0, 0).

Theta - Line rotation angle in radians, specified as a real, 2-D, non-sparse logical or numeric array.

It generates the Rho and Theta axial plot:

```
>> imshow(H,[],'XData',T,'YData',R,...
'InitialMagnification','fit');
>> xlabel('\theta'), ylabel('\rho');
>> axis on, axis normal, hold on;

>> P = houghpeaks(H,25,'threshold',ceil(0.3*max(H(:))));
>> x = T(P(:,2)); y = R(P(:,1));
>> plot(x,y,'s','color','white');
>> lines = houghlines(BW,T,R,P,'FillGap',10,'MinLength',15);
>> figure, imshow(I), hold on;
```

Here, peaks means Row and column coordinates of Hough transform bins, specified as a real, non-sparse numeric array. FillGap means distance between two line segments associated with the same Hough transform bin, specified as a positive real scalar. When the distance between the line segments is less than the value specified, the Hough lines function merges the line segments into a single line segment. Here, the value for 'FillGap' has been assigned as 10.

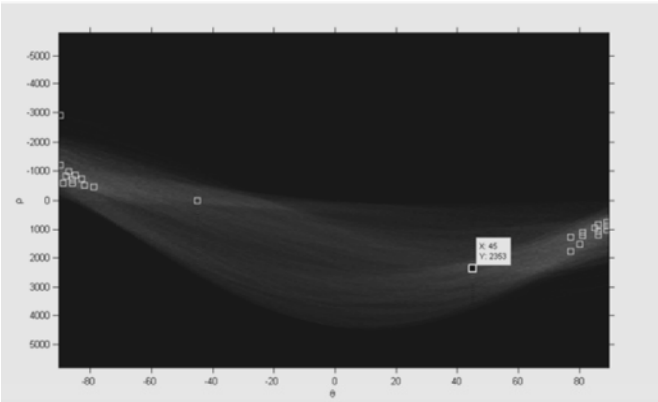

Fig.3. Plot on theta and rho axial plane with the peak values.

MinLength means minimum line length, specified as a positive real scalar. Hough lines discard lines that are shorter than the value specified. 15 pixels have been taken in this work as 'MinLength'.

This code will show the peaks in the plot (Fig.3), on the basis of which, the points will be joined as line or the target lineaments.

```
for k = 1:length(lines)
xy = [lines(k).point1; lines(k).point2];
plot(xy(:,1),xy(:,2),'LineWidth',2,'Color','green');
plot(xy(1,1),xy(1,2),'x','LineWidth',2,'Color','yellow');
plot(xy(2,1),xy(2,2),'x','LineWidth',2,'Color','red');
len = norm(lines(k).point1 - lines(k).point2);
```

Verification with Respect to Landslides

A comparative analysis between the outputs generated from LINE method as well as Hough transformation method was done with respect to the rose diagrams as well as the lineament density maps. The directional analysis from the rose diagrams built on three output lineaments in the study was verified with the lithological structure of Darjeeling district. It was followed by the relational analysis of the high density zones with that of the existing landslides from the landslide inventory map. It gives an idea on the accuracy of the processes of automated mapping of lineament and the data input involved, which is an influential factor behind landslide occurrence.

RESULTS AND DISCUSSION

Stacking of 9 bands of Landsat-8 OLI came out with a single output image which was used for information extraction. Information is mainly on the contrasting pixels in a continuous linear pattern of specified length. For the purpose, principal component analysis was applied. It runs to identify patterns in data and expressing the data in such a way as to highlight their similarities and differences. The first PCA (Fig. 4a) is the linear combination of x-variables that has maximum variances among all linear combinations. So, it accounts for as much variation in the data as possible. This led the author to work with forward PCA on Landsat-8 OLI. It generated the output image with maximum possible variance in n-dimensional band data scatter plots. This output image was suitable to run through LINE algorithm in PCI-Geomatica, as it could extract edges as lineaments (Fig.4b).

The same anomaly detection was targeted to run through LINE where the data source was digital elevation model. Here, edge enhancement and detection was done by hill shading analysis as the source datasets here is the matrix of elevation data instead of ground reflection. The output image generated was an image with enhanced edges from a specific viewpoint. Here the illumination directions of 180, 225, 270 and 315 angles were taken as the viewpoints (Fig. 5a-d). Hence combining these four shaded relief images, an output image (*Figure: 5e*) was generated which enhanced drastic variation in

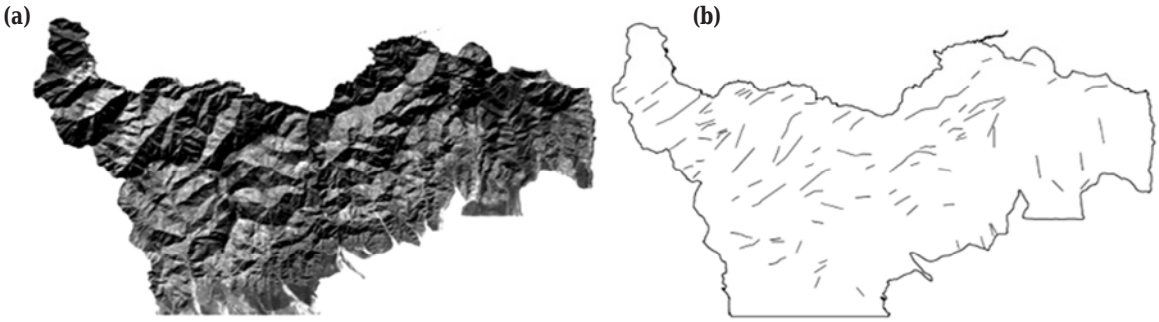

Fig.4. (a) First Principal Component Analysis on Landsat-8 OLI. **(b)** Limeament output from PCA by LINE menthod.

elevation as viewed from the western quadrant. This output was then used as the input for LINE process to derive lineaments (Fig.5f).

Hence, these two output lineament data, which are the results of LINE algorithm though from two different source data types, were tested to get effectiveness of automatic lineament extraction process and data source with reference to landslide hazard. As lineaments are the lithologically weaker zones, it boosts land sliding. Hence the existing landslides are supposed to be concentrated within the higher lineament density zones. To develop a neutral platform of analysis, these two output lineament vectors were processed to get density rasters with same pixel size and sliced into four ranges. It was evaluated that, out of 123 existing landslides as depicted from landslide inventory map of Darjiling district administration *(http://wbdmd.gov.in/Pages/Land_Mapping.aspx)*, 58 comes under the first two categories with higher values in the density raster (Fig.7b*)* generated from landsat-8 OLI lineaments with an accuracy of 47%. For the DEM data extracted lineaments, the density raster (Fig.7a*)* giving the statistics is 21 with an accuracy of only 17%. Now, it can be said that, in this LINeament Extraction process (LINE), Landsat-8 OLI is performing better than that of DEM.

But the accuracy achieved from Landsat-8 OLI data source is not enough satisfactory. Therefore, this data source was tested in another algorithm i.e. the Hough transformation, which was run through MATLAB coding. It applied Canny's edge detection on the image. It generated the binary edge data (Fig.6a*)* which was analyzed in the Hough space for its edge pixels with reference to two parameters, rho

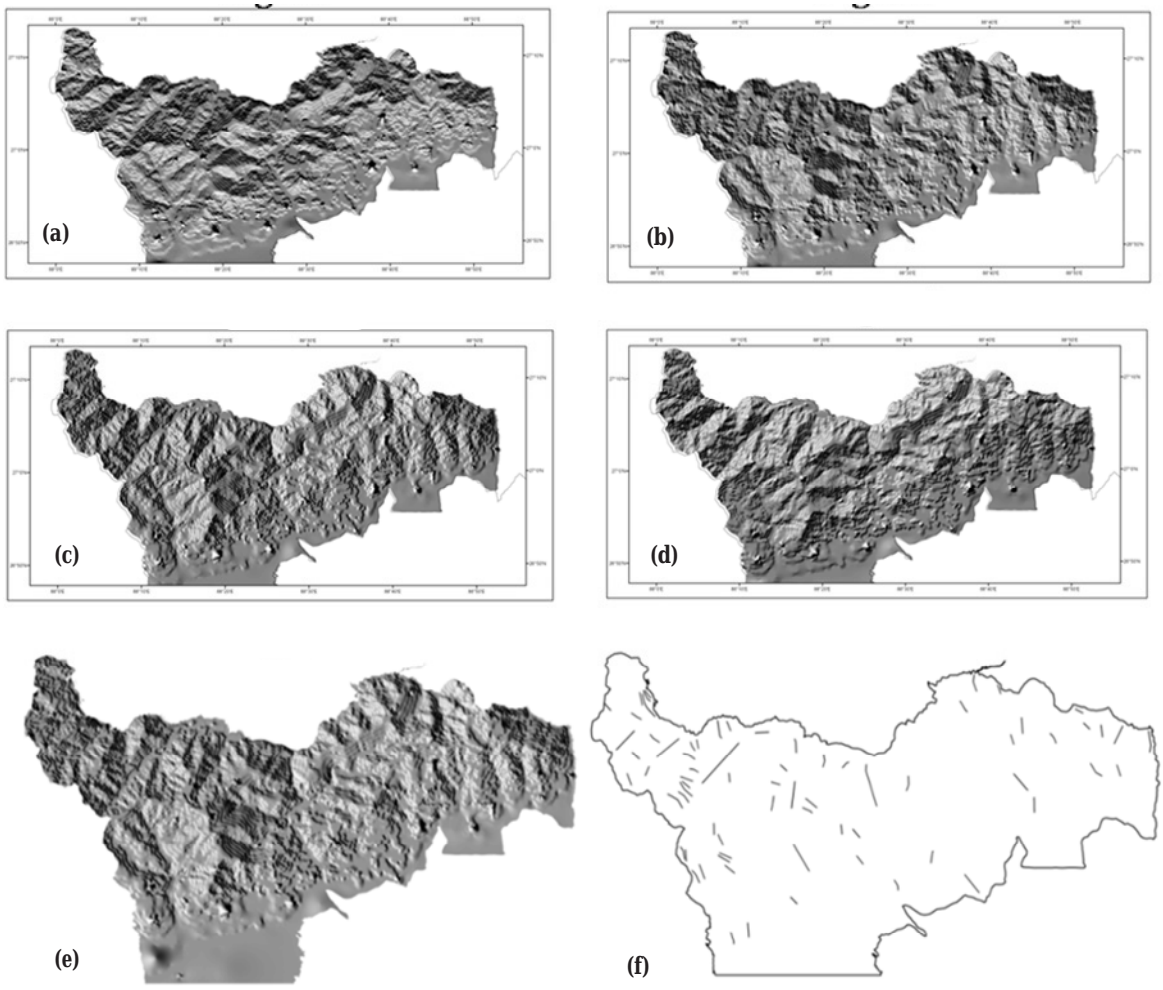

Fig.5. (a) Hill shade of 180°, **(b)** Hill shade of 225°, **(c)** Hill shade of 270°, **(d)** Hill shade of 315°, **(e)** combined hill shade image, **(f)** Output lineaments by LINE tool in PCI-Geomatica.

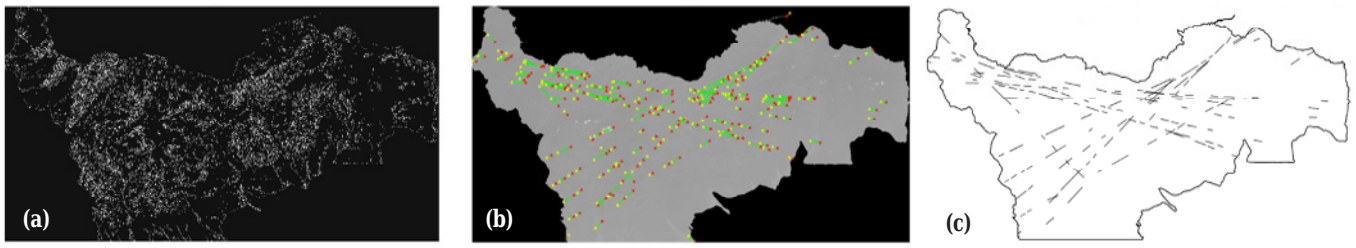

Fig.6. (a) Binary image derived from Canny edge enhancement, **(b)** Output lineaments after running Hough transformation, **(c)** Output vector lineaments generated by Hough transformation method.

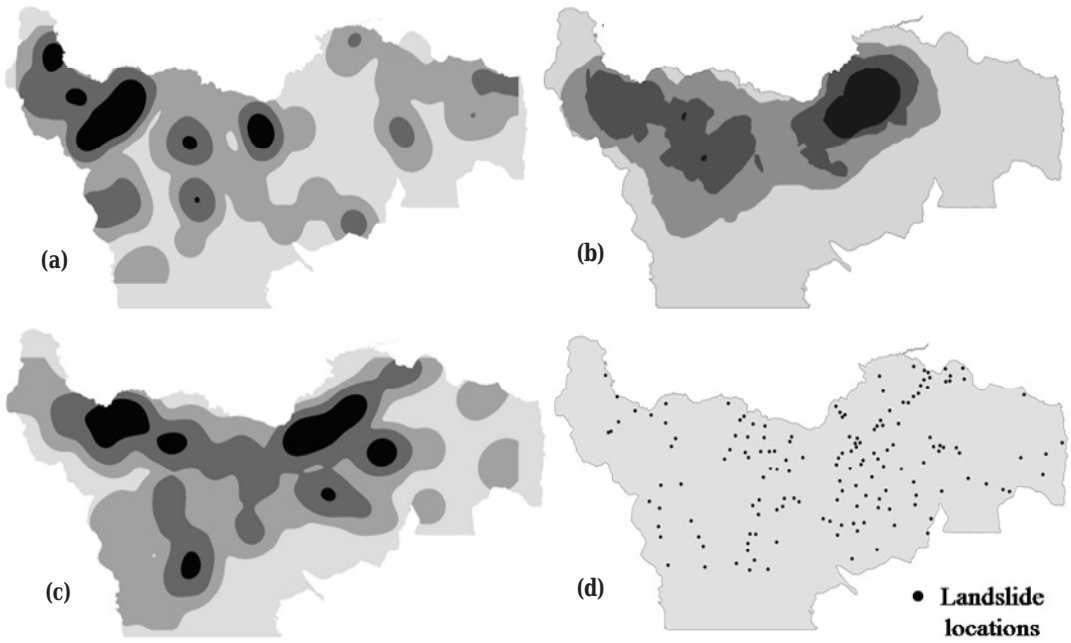

Fig.7. (a) Lineament density map from DEM by LINE method, (b) Lineament density map from Landsat-8 OLI by LINE method, (c) Lineament density map from Landsat-8 OLI by Hough Transformation method, (d) Already occurred landslides in Darjeeling district.

and theta (Fig.3). So, all data plotted in the scatter diagram with these two parameters in x and y axis showed the peak values. As per the assigned fill-gaps and min-length, spatial linearity in the data anomaly was detected (Fig.6b*)*. This was processed to transform into vector lineaments (Fig.6c*)*. The density of this lineament was calculated which shows that out of 123 landslides, 74 landslides are coming under first two higher density classes (Fig.7c*)*. Hence, the accuracy is coming as 60%. Therefore, Hough transformation seems to perform better in case of algorithm based automated lineament detection system.

Though this method was proved to be nearest to reality, the patterns of the lineaments were quite uncommon and the lines were placed in the whole state as the letter 'X' (Fig.8*)*. Then, the lithological structure of the area was referred and it was seen that the main central thrust zone is place in a similar way. So, a need for analyzing the lineaments in term of their direction was realized. For the purpose, the directions of the lineaments in percentage of total were represented as rose diagrams in Rockworks software (Fig.9a-d). The accuracy checking in this case was conducted with reference to the rose plot drawn on lithological stratigraphy of the study area.

Here also, it can be seen that the best matching of directional frequency of lineaments are in between the stratigraphy and the lineaments derived from Hough transformation on Landsat-8 OLI.

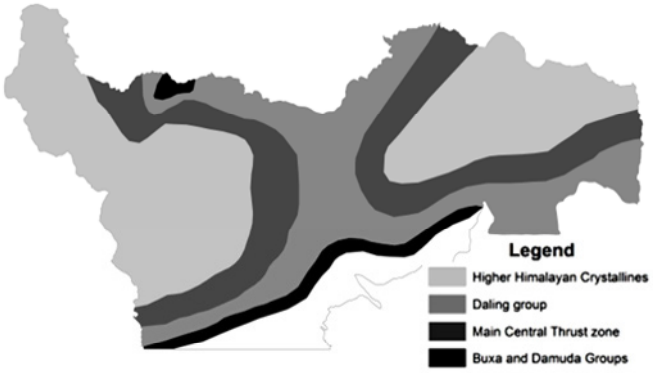

Fig.8. Geological set up of the study area (source: Acton et al., 2011)

CONCLUSION

This paper deals with the review of the methodologies as well as data sources involved in automated lineament extraction. As per the data source is concerned, ground reflection data performs better than that of ground elevation data. Whereas, in case of methodologies concerned, Hough transformation with parameterization of each data was proved to be better than LINE algorithm of PCI Geomatica. The extracted lineaments derived by Hough transformation, are correlative with the geological set up. Here, the mapping and interpretation of tectonic lineaments is very complex which requires the inspection and integration of the geological and geomorphological features of the target area. The accuracy in terms of landslide occurrences is also high enough. Lineament density is one of the factors that lead to this hazard. So, a low percentage of landslides occurring within the higher lineament density zone may be due to other instigating factors.

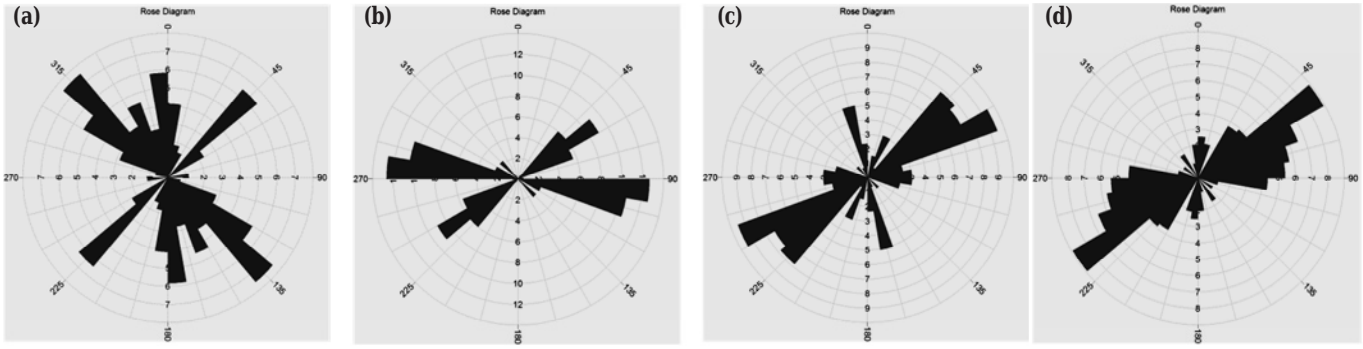

Fig.9. Rose diagrams on frequency of directions of lineaments derived from **(a)** DEM by LINE, **(b)** Landsat-8 OLI by LINE, **(c)** Landsat-8 OLI by Hough Transformation, **(d)** Geological central thrust boundary

Therefore, the percentage of accuracy should be ignored though the comparative evaluation should only be considered.

References

Abarca, M.A.A (2006) Lineament extraction from digital terrain models, case study: San Antonio del sur area, South-eastern Cuba", thesis submitted to the International Institute for Geoinformation Science and Earth Observation, ITC, The Netherlands. Accessed from: *https://www.itc.nl/library/papers_2006/msc/ereg/arenas.pdf* on 9th April, 2017.

Abdullah, A. Nassr, S. and Ghaleeb, A. (2013) Landsat ETM-7 for lineament mapping using automatic extraction technique in the SW part of Taiz area, Yamen", Global Journal of Human Social Science, vol. 13(3). Accessed from *https://globaljournals.org/GJHSS_Volume 13/5-Landsat-ETM-for-Lineament-Mapping.pdf* on 11th March, 2017.

Acton, C.E., Priestley, K., Mitra, S., Gaur, V.K. (2011) Crustal structure of the Darjeeling—Sikkim Himalaya and southern Tibet. Internat. Jour. Geophys., v.184(2), pp.829-852.

Albanagan, R., Rohan K., Lakshmanan, K., Parida, S. and Neethu, S. (2015) Landslide hazard zonation mapping using frequency ratio and fuzzy logic approach, a case study of Lachung Valley, Sikkim. Geoenvironmental Disasters, v.2(6), pp.3-17.

Alhirmizy, S (2015) Automatic mapping of lineaments using shaded relief images derived from Digital Elevation Model (DEM) in Kirkuk Northeast Iraq. Internat. Jour. Sci. Res., v.4(5), pp.2228-2233.

Argialas, D.P. and Mavrantza, O.D. (2004) Comparison of Edge Detection and Hough Transform Techniques in Extraction of Geologic Features. *In:* Proc. XXth ISPRS Congress of the International Society of Photogrammetry and Remote Sensing, 12-23 July 2004, Turkey, IAPRS-XXXV, pp.790-795.

Auden, J.B. (1935) Traverses in the Himalaya. Rec. Geol. Surv. India, LXIX (part-2), pp.123-167.

Ballard, D.H. and Brown, C.M. (1982) Computer Vision. Prentice Hall Inc., Englewood Cliffs, New Jersey, pp.123-131.

Canny, J. F. (1986) A computational approach to edge detection. IEEE Trans. on Pattern Analysis and Machine Intelligence, v.8, pp.679-714.

Dalati, M. (2000) Lineaments on Landsat images – detection mapping and tectonic significance in north-western depressions of Syria. International Archives of Photogrammetry and Remote Sensing, v.33(B7), pp.301-305.

Dash, A.J. (1947) Bengal District Gazetteers, Darjeeling, Bengal Government Press, Alipore, Bengal,

Duda, R.O. and Hart, P.E. (1972) Use of the Hough Transform to detect curves and lines in pictures. Communications of the Association for Computing Machinery, v.15(1), pp.11-15.

El-sawy K. El-sawy, Atef, M. Ibrahim, Mohamed A. El-bastawesy and Waleed A. El-saud (2016) Automated, manual lineaments extraction and geospatial analysis for Cairo-Suez district (Northeastern Cairo-Egypt), using remote sensing and GIS. Internat. Jour. Innovative Sci., Engg. and Tech., v.3(5), pp.491-500.

Fitton, N.C. and Cox, S.J.D. (1998) Optimizing the application of the hough transformation for the automated feature extraction from geoscientific images. Computers and Geosciences, v.24, pp.933-951.

Gupta, R.G (1991) Remote Sensing geology. Springer-Verlag, Berlin, 356p.

Hassan, M.A. and Adhab, S.S. (2014) Lineament automatic extraction analysis for Galal Badra river basin using Landsat 8 satellite image. Iraqi Jour. Physics, v.12(25), pp.44-55.

Hobbs, W.H. (1911) Repeating patterns in the relief and in the structure of the land. Geol. Soc., v.22, pp.123–176.

Hough, P.V.C. (1962) Method and means for recognizing complex patterns. U.S. Patent 3,069,654.

Ibrahim, U and Mutua, F. (2014) Lineament extraction using Landsat 8 (OLI) in Gedo, Somalia. Internat. Jour. Sci. Res., v.3(9), pp.291-296.

Karnieli, A., Meisels, A., Fisher, L. and Arkin, Y. (1996) Automatic extraction and evaluation of geological linear features from digital remote sensing data using Hough Transformation. Photogrammetric Engineering & Remote Sensing, v.62(5), pp.525-531.

Kocal, A., Duzgun, H.S. and Karpuz, C. (2004) Discontinuity mapping with automatic lineament extraction from high resolution satellite imagery", ISPRS Proc.-XXXV. Accessed from: *www.isprs.org/proceedings/XXXV/congress/comm7/papers/205.pdf*. on 27th March, 2017.

Mallet, F.R. (1875) On the geology and mineral resources of the Darjiling District and the Western Duars. Geol. Surv. India Mem., v.11 pp.1–50.

Mandal, S. and Maiti, R. (2014) Role of lithological composition and lineaments in landsliding: A case study of Shivkhola watershed, Darjeeling Himalaya. Internat. Jour. Geol. Earth and Environ. Sci., v.4(1), pp.126-132.

Mankisch, M., Stotter, J., Monteferri, F.P. and Rutzinger, M. (2007) Algorithms for the extraction of lineaments from airborne laser scanning data. Institute of Mountain Research, accessed from *http://www.zobodat.at/pdf/IGF-Forschungsberichte_2_0371-0378.pdf* on 14th February, 2017.

Masoud, A.A and Koike, K. (2011) Auto-detection and integration of tectonically significant lineaments from SRTM DEM and remotely sensed geophysical data. ISPRS Jour. Photogrametry and Remote Sensing, v.66, pp.818-832.

Matori, A.N., Basith, A. and Harahap, I.S.H. (2012) Study of regional monsoonal effects on landslide hazard zonation in Cameron Highlands, Malaysia. Arabian Jour. Geosci., v.5(5), pp.1069–1084.

Mishra, O.P. (2014) Intricacies of the Himalayan seismotectonics and seismogenesis: need for integrated research. Curr. Sci., v.106(2), pp.176-187.

Morris, K. (1991) Using knowledge-base rules to map the three dimensional nature of geologic features. Photogrammetric Engineering and Remote Sensing, v.57, pp.1209-1216.

Neawsuparp, K. and P. Charusiri, (2004) Lineaments Analysis Determined from Landsat Data Implication for Tectonic Features and Mineral Occurrences in Northern Loei Area, NE Thailand. Science Asia, v.30, pp.269-278.

Prasad, A.D., Jain, K. and Gairola, A. (2013) Mapping of lineaments and knowledge base preparation using geomatics techniques for part of the Godavari and Tapi basins, India: a case study. Internat. Jour. Computer Applications, v.70(9), pp.39-47.

Rahnama, M. and Gloaguen, R. (2014) Techlines: A MATLAB based toolbox for tectonic lineament analysis from satellite images and DEMs, Part-1: Line segment detection and extraction. Remote Sensing, v.6, pp.5938-5958.

Rahnama, M. and Gloaguen, R. (2014) Techlines: A MATLAB based toolbox for tectonic lineament analysis from satellite images and DEMs, Part-2: Line segment linking and merging. Remote Sensing, v.6, pp.11468-11493.

Shankar, B., Tornabene, L.L., Osinski, G. R., Roffey M., Bailey, J. M. and Smith, D. (2016) Automated lineament extraction technique for the Sudbury impact structure using remote sensing datasets – an update. 47th Lunar and Planetary Science Conference, Accessed from: *https://www.hou.usra.edu/meetings/lpsc2016/pdf/1424.pdf* on 7th April, 2017.

Šilhavi, J., Minár J., Mentlík, P. and Sládek, J. (2016) A new artefacts resistant method for automatic lineament extraction using Multi-hillshade Hierarchic Clustering (MHHC). Computers and Geosciences, v.92, pp.9-20.

Thannoun, R.G. (2013) Automatic Extraction and Geospatial Analysis of Lineaments and their Tectonic Significance in some areas of Northern Iraq using Remote Sensing Techniques and GIS. Internat. Jour. Enhanced Res. Sci. Tech. Engg., v.2(2), pp.1-11.

Wang, J. and Howarth, P.J (1990) Use of the hough transformation in automated lineament detection. IEEE Trans. Geoscience and Remote Sensing, v.28, pp.561-566.

Zheng, X., Xiong, H., Yye, L. and Gong, J. (2016) An improved ANUDEM method combining topographic correction and DEM interpolation. Geocarto Internat., v.31(5), pp.492-505.

http://darjeeling.gov.in/geography.html accessed on 2nd February, 2017

http://wbdmd.gov.in/Pages/Land_Mapping.aspx accessed on 2nd February, 2017

https://in.mathworks.com/help/images/ref/hough.html?requestedDomain=in.mathworks.com accessed on 17th April, 2017.

http://pro.arcgis.com/en/pro-app/too-reference/3d-analyst/how-topo-to-raster-works.htm. accessed on 5th March, 2017.

www.pcigeomatics.com/TrainingGuide-Geomatica-1.pdf accessed on 23rd March, 2017.

(Received: 4 August 2017; Revised form accepted: 4 November 2017)